Coulomb drag of edge excitations in the Chern-Simons theory of the fractional quantum Hall effect

Dror Orgad and Shimon Levit

Department of Condensed Matter, The Weizmann Institute of Science, Rehovot 76100, Israel

Long-range Coulomb interaction between the edges of a Hall bar changes the nature of the gapless edge excitations. Instead of independent modes propagating in opposite directions on each edge as expected for a short-range interaction one finds elementary excitations living simultaneously on both edges, i.e., composed of correlated density waves propagating in the *same direction* on opposite edges. We discuss the microscopic features of this Coulomb drag of excitations in the fractional quantum Hall regime within the framework of the bosonic Chern-Simons Landau-Ginzburg theory. The dispersion law of these excitations is nonlinear and depends on the distance between the edges as well as on the current that flows through the sample. The latter dependence indicates a possibility of parametric excitation of these modes. The bulk distributions of the density and currents of the edge excitations differ significantly for short- and long-range interactions.

I. INTRODUCTION

The integer and fractional quantum Hall effects (QHE) occur in a two-dimensional electron gas placed in a strong perpendicular magnetic field. Interesting phenomena can take place at the edges of this gas. The simplest is related to the edge currents that are instrumental in our understanding of the transport properties of the QHE.[1–4] The character of the excitations in the quantum Hall system is also effected by the presence of the edges. While the bulk excitations have a finite gap the excitations that are localized near the edges are found to be gapless. They are chiral, that is moving only in one direction along the edge, and can be described by the chiral Luttinger model[5] provided one disregards their coupling to other modes. Recently the possibility to probe the structure of the fractional Hall states by studying the tunneling between edges attracted much attention.[6,7]

In this paper we study the edge excitations within the framework of a bosonic Chern-Simons Landau-Ginsburg (CSLG) theory. This theory[8] was proposed as a useful supplement and extension of Laughlin's fully microscopic many-body theory of the fractional QHE (FQHE). Recently, the edge effects were studied using this theory[9] and Wen's results were rederived. Our goal is to investigate the effects of the interedge interactions. In Ref. 10 unusual effects were predicted due to this interaction that are related to the redefinition of the gapless modes into a Bogoliubov transformed combination of modes living on both edges and propagating in the same direction. Our analysis goes one step further and presents the microscopic picture of this phenomenon. We use the realistic Coulomb interaction between the edges and derive the modified modes and their density and current distributions. These clearly indicate that one deals with the Coulomb drag of excitations on one edge by the other. We derive a nonlinear dispersion relation for the modified excitation modes and find that it depends on the width of the Hall bar and on the total current that flows through it. We point out that the latter dependence opens the possibility of a parametric excitation of these modes.

II. STATIC SOLUTIONS FOR A SINGLE EDGE

The starting point of our analysis is the mean-field equations derived by minimizing the CSLG action for the fractional quantum Hall effect.[8] Using the polar decomposition of the bosonic field $\phi = \sqrt{\rho} e^{i\theta}$ and introducing the velocity fields

$$v_i = \frac{\hbar}{m} \partial_i \theta + \frac{e}{mc}(a_i + A_i),$$ (1)

with the vector potential **A** taken such as to produce a constant magnetic field along z, one obtains the hydrodynamic form of these equations, which is more convenient for our purpose,

$$\epsilon_{ij}\partial_i v_j = 1 - \rho,$$ (2a)

$$\partial_t \partial_i \theta - \partial_t v_i - \partial_i a_0 = \epsilon_{ij}\rho v_j,$$ (2b)

$$\partial_t \rho = -\partial_i(\rho v_i),$$ (2c)

$$\partial_t \theta = -\frac{1}{2}v_i^2 + \frac{1}{2}\frac{\partial_i^2 \sqrt{\rho}}{\sqrt{\rho}} + a_0 - V(x) - \rho$$

$$-\frac{\nu}{2\pi}\int U(\mathbf{r}-\mathbf{r}')\rho(\mathbf{r}')d^2\mathbf{r}'.$$ (2d)

Here and throughout the paper length is measured in units of the magnetic length $l = \sqrt{\hbar c/eB}$, time in units of inverse cyclotron frequency $\omega_c = eB/mc$, energy is normalized by $\hbar\omega_c$, and the density by its bulk value $\bar{\rho} = \nu B/\phi_0$, where $\nu = 1/(2n+1)$ is the filling factor. All the quantities apart of θ and a_0 are gauge invariant and the latter appear in the gauge invariant combination $\partial_t \theta - a_0$. In order to correctly reproduce the energetics of the noninteracting limit we have followed Ref. 11 and included a δ-function type repulsive force [the term before the last in (2d)] with a strength of $2\pi\hbar^2/\nu m$. Our confining potential is assumed to rise fast enough to avoid the occurrence of an alternating sequence of
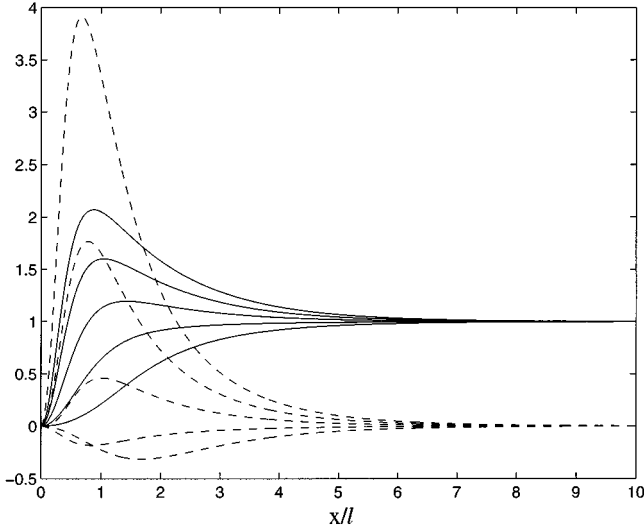
FIG. 1. Density in units of $\bar{\rho}$ (solid lines) and current density in units of $\bar{\rho}\omega_c l$ (dashed lines) for the case of short-range interaction with $\lambda_s = 1$. The highest curve in each set corresponds to $x_0 = -2$. Consecutive curves differ by $\Delta x_0 = 1$. The reversal in the direction of the current with increasing x_0 manifests a transition from skipping orbits to circular orbits on the rim of the Hall drop.

compressible and incompressible strips along the edge.[3,4] Apart from this requirement the detailed nature of $V(x)$ is of no importance for our applications.

Our aim is to obtain the edge excitations as the random phase approximation (RPA) modes of the theory, i.e., the eigenmodes of the above equations linearized around a static solution. We first consider a single edge. The translation invariance in the y direction suggests looking for a static solution in the form

$$\theta = -x_0 y - \mu(x_0)t, \quad \rho = \rho(x), \quad v_x = 0, \quad v_y = v_y(x),$$

$$a_0 = a_0(x). \tag{3}$$

We assume for definiteness an infinitely high wall situated at $x \leq 0$ and accordingly set the density to zero at the wall. The only gauge freedom that preserves the form of the above solution is adding arbitrary constants to x_0 and μ. We fix this freedom by requiring that the statistical potentials a_0, a_i vanish at $x = 0$ and choosing $\mathbf{A} = (0, Bx, 0)$. This assures that solutions with different values of x_0 and μ are not gauge transforms of each other. Formally x_0 is the conserved momentum along the edge and its physical effect on the condensate ϕ is similar to the guiding center coordinate of Landau levels—changing its value translates ϕ in the x direction. Inserting the ansatz (3) into (2a)–(2d) one finds a set of coupled equations for $\rho(x)$, $v_y(x)$, and $a_0(x)$ that we have solved numerically. For a fixed x_0 we have determined the value of μ by requiring that ρ approaches $\bar{\rho}$ far from the edge. Under this condition μ is the energy that is needed in order to add a particle to the edge. Representative examples of the density and current density profiles for solutions (3) in the case of short-range interactions $U = (2\pi\hbar^2\lambda_s/\nu m)\delta(\mathbf{r} - \mathbf{r}')$ are shown in Fig. 1. One finds a *one-parameter family of static solutions* depending on x_0 and differing by the density of particles at the edge. Inserted in
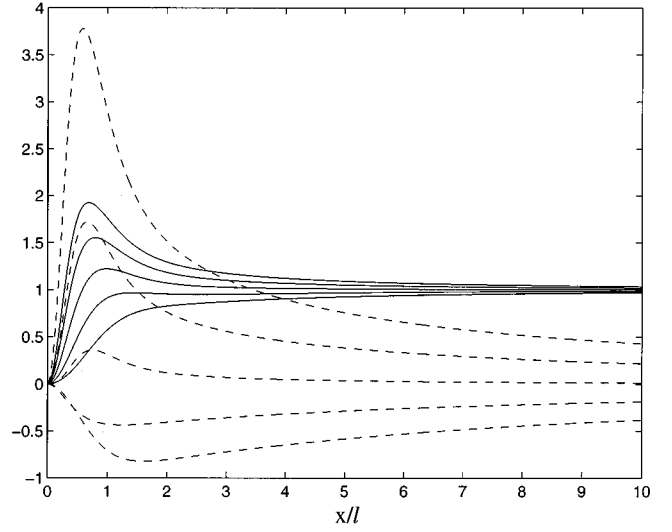

FIG. 2. Same as Fig. 1 for Coulomb interaction with $\lambda_c = 1$.

(1) our boundary conditions and the ansatz (3) give the velocity at the edge as $v_y(0) = -x_0$. Using this and the fact that the velocity falls to zero in the bulk we integrate Eq. (2a) and find that $-x_0$ is the *excess charge* per unit length along the edge relative to a steplike constant density profile.

For a Coulomb interaction $U = 2\pi\nu^{-1}\lambda_c\hbar\omega_c/|\mathbf{r} - \mathbf{r}'|$ with $\lambda_c = \nu e^2/2\pi\epsilon l\hbar\omega_c$ and a constant neutralizing background extending up to the wall one obtains distributions shown in Fig. 2. Compared to Fig. 1 the essential difference is found in the large-x behavior of the solutions. Inserting the following asymptotic forms for large x,

$$\rho(x) \simeq 1 - \text{sgn}(x_0)\exp(-\alpha x),$$

$$v_y(x) \simeq -\text{sgn}(x_0)\alpha^{-1}\exp(-\alpha x), \tag{4}$$

$$a_0(x) \simeq -\mu + \lambda_c + 1 - \text{sgn}(x_0)\alpha^{-2}\exp(-\alpha x),$$

into Eqs. (2a)–(2d) one finds for the short-range interaction that $\alpha = [2(\lambda_s + 1) - 2\sqrt{(\lambda_s + 1)^2 - 1}]^{1/2}$. For the Coulomb interaction the fields behave at large distances according to

$$\rho(x) \simeq 1 - 2\lambda_c x_0/x^2,$$

$$v_y(x) \simeq -2\lambda_c x_0/x, \tag{5}$$

$$a_0(x) \simeq -\tilde{\mu} + 1 + 2\lambda_c x_0 \ln(x).$$

These expressions exhibit a significant difference in the bulk distribution of the current $J_y(x) = \rho(x)v_y(x)$ for short-range and Coulomb interactions. In deriving these results we assumed that the length of the sample L is very large compared to x_0 and used the fact that the density of the solutions considered here does not depend on the coordinate along the edge. Under such conditions one can integrate over the y coordinate in the interaction term to find $\nu/2\pi \int U(\mathbf{r} - \mathbf{r}')[\rho(\mathbf{r})' - 1]d^2\mathbf{r}' \simeq -2\lambda_c x_0 \ln L - 2\lambda_c \int [\rho(x') - 1]\ln(|x - x'|)dx'$. The first term is a constant that is absorbed into the chemical potential while the second one is a potential of a collection of charged wires.

An even more pronounced difference is found in the dependence of μ on x_0, which is displayed in Fig. 3. Numeri-
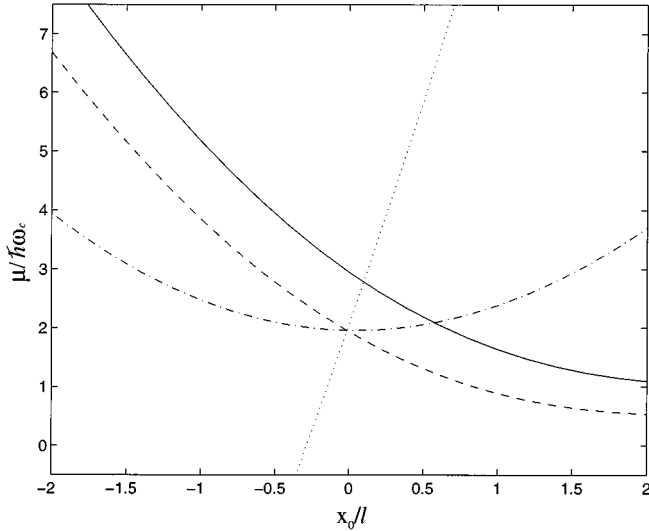
FIG. 3. The chemical potential at the edge as a function of x_0 for short-range interaction with $\lambda_s = 1$ (solid line). For the Coulomb interaction we plot $\tilde{\mu} = \mu + 2\lambda_c x_0 \ln L$ in the case $\lambda_c = 0.03$ (dashed line), which corresponds to the FQH regime and for comparison also the cases $\lambda_c = 1$ (dashed-dotted line) and $\lambda_c = 3$ (dotted line), which may be relevant to integer quantum Hall samples.

cally we find that for the short-range interaction the chemical potential tends to $\frac{1}{2}(\lambda_s + 1)$ for large positive values of x_0 and increases as the charges are pushed against the wall, i.e., for decreasing x_0. In the case of the Coulomb interaction the leading contribution to μ is given by $-2\lambda_c x_0 \ln L$. This term corresponds to the electrostatic charging energy of the excess charge ($-x_0$) had it been uniformly distributed over a strip of width l along the edge. Its change of sign at $x_0 = 0$ reflects the tendency of the system to remain neutral. The remaining part of the chemical potential $\tilde{\mu} = \mu + 2\lambda_c x_0 \ln L$ is due to the kinetic energy and the deviation of the excess charge distribution from that of a uniform strip. As one can observe from Fig. 3 the dependence of $\tilde{\mu}$ on x_0 varies considerably as the strength of the interaction is changed.

III. EXCITATIONS OF A SINGLE EDGE

Linearizing Eqs. (2a)–(2d) around one of the solutions (3) we obtain the RPA equations

$$\epsilon_{ij}\partial_i \delta v_j = -\delta\rho, \tag{6a}$$

$$\partial_t \partial_i \delta\theta - \partial_t \delta v_i - \partial_i \delta a_0 = \epsilon_{iy} v_y \delta\rho + \epsilon_{ij} \rho \delta v_j, \tag{6b}$$

$$\partial_t \delta\rho = -v_y \partial_y \delta\rho - \partial_i(\rho \delta v_i), \tag{6c}$$

$$\partial_t \delta\theta = -v_y \delta v_y + f(\rho, \delta\rho) + \frac{\partial_y^2 \delta\rho}{4\rho} + \delta a_0 - \delta\rho$$
$$- \frac{\nu}{2\pi} \int U(\mathbf{r} - \mathbf{r}') \delta\rho(\mathbf{r}') d^2\mathbf{r}', \tag{6d}$$

where f denotes the part of the linearized "quantum pressure" term, i.e., the second term on the right-hand side of (2d), containing x derivatives.
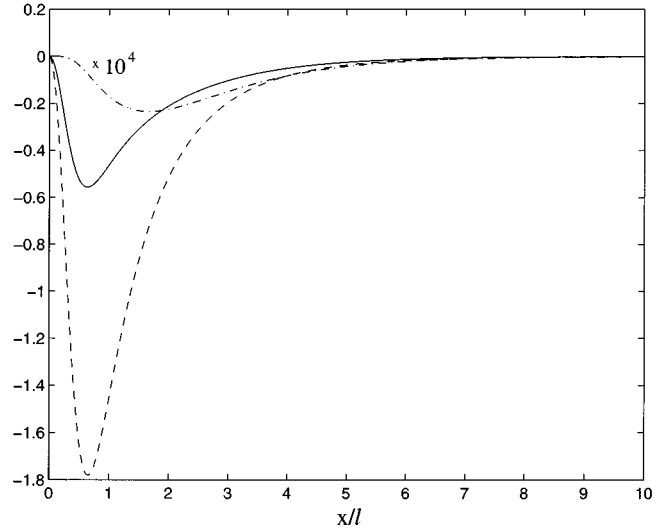

FIG. 4. Profiles of density (solid line), current density in the y direction (dashed line), and current density in the x direction (dashed-dotted line) for gapless edge excitations in the case of short-range interaction with $\lambda_s = 1$. The profiles shown here are around a static solution with $x_0 = -1$ and with $kl = 10^{-4}$. The density is normalized by $\bar{\rho}$, the current densities by $\bar{\rho}\omega_c l$, and δJ_x is multiplied by $k^{-1} = 10^4$.

Our main method of solving Eqs. (6a)–(6d) will be to use the continuous one-parameter family of static solutions described above in order to find the *gapless* branch of the RPA eigenmodes. The derivative of the solution (3) with respect to x_0 constitutes a static solution of the RPA equations (6a)–(6d). Motivated by this observation and concentrating on the long-wavelength limit we set

$$\delta\rho = \partial_{x_0}\rho(x)\cos(ky - \omega t),$$

$$\delta v_y = \partial_{x_0} v_y(x)\cos(ky - \omega t),$$

$$\delta a_0 = \partial_{x_0} a_0(x)\cos(ky - \omega t),$$

$$\delta\theta = -\frac{1}{k}\sin(ky - \omega t). \tag{7}$$

Clearly these density and velocity distributions are concentrated along the edge as illustrated in Figs. 4 and 5. As can be seen by differentiating Eqs. (4) and (5) with respect to x_0, for short-range interaction these distributions decay exponentially into the bulk, while for the Coulomb interaction the decay follows a power law. With the expression (8) for ω given below also the gauge invariant combination $\partial_t \delta\theta - \delta a_0$ vanishes far away from the edge. Inserting these functions into Eq. (6d), using the fact that their x-dependent parts are static solutions and neglecting the term proportional to k^2 we find that they indeed solve this equation, provided we choose properly the dispersion relation $\omega = \omega(k)$. In the case of the short-range interaction we find directly

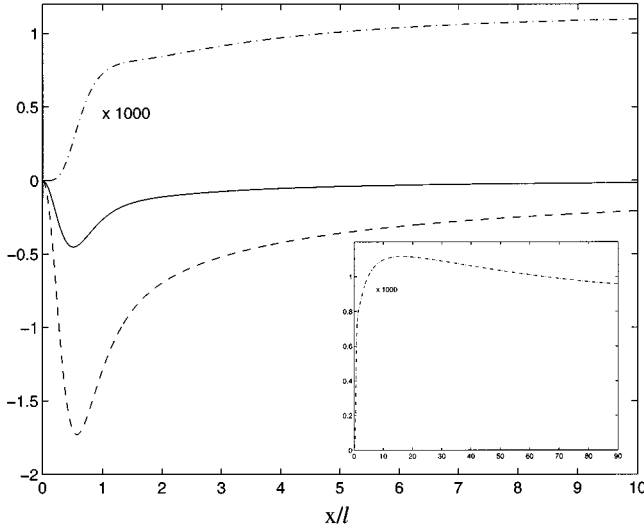$$\omega = -\frac{l^2}{\hbar}\frac{\partial\mu}{\partial x_0}k(1 + kl), \tag{8}$$

FIG. 5. Same as Fig. 4 for Coulomb interaction with $\lambda_c = 1$. The inset shows the behavior of δJ_x at larger distances from the wall. δJ_x is multiplied by $k^{-1}/10 = 10^3$.

where we have restored the units of dimensions. In this expression we have included the second-order term in k, which can be obtained after multiplying the first three fields in (7) by $1 + kl$. In the case of the Coulomb interaction after the substitution of $\delta\rho$ the last term in Eq. (6d) becomes $-2\lambda_c \cos(ky - \omega t) \int_0^\infty dx' \partial_{x_0} \rho(x') K_0(|k||x-x'|)$ where $K_0(x)$ is the modified Bessel function. Working in the region $x \ll k^{-1}$ and assuming that k^{-1} is much larger than the width of the region where $\partial_{x_0}\rho$ is appreciable we can use the approximation $K_0(|k||x-x'|) \approx \ln(2e^{-\gamma}/|k||x-x'|)$ where γ is the Euler constant. As a result we find that Eq. (6d) is satisfied to first order in k when the dispersion law is modified by an extra logarithmic term, cf. Refs. 12 and 13,

$$\omega = -\frac{l^2}{\hbar}\frac{\partial\tilde{\mu}}{\partial x_0}k + \frac{\nu}{\pi}\frac{e^2}{\epsilon\hbar}k\ln\left(\frac{2e^{-\gamma}}{|k|l}\right). \qquad (9)$$

Note that $\tilde{\mu}$ rather then μ (cf. Fig. 3) enters this expression since only the logarithmic part of the interaction term is present in this case.

Turning now to the linearized continuity equation (6c) we find that in order to solve it the solution (7) should be supplemented by a velocity field in the x direction:

$$\delta v_x = \frac{1}{\rho}(\omega\partial_{x_0}v_y - k\partial_{x_0}a_0 + \omega)\sin(ky - \omega t). \qquad (10)$$

The corresponding current density $\delta J_x = \rho\delta v_x$ is of order k as compared to the current density δJ_y. Using the boundary conditions and the asymptotic behavior (4) of the fields for short-range interaction it is easy to check that this current vanishes on the wall ($x = 0$) as well as far away from it ($x \rightarrow \infty$). For the Coulomb interaction this expression for the velocity is accurate only for $x \ll k^{-1}$. Although it vanishes on the wall it has a long tail $2\lambda_c k \ln(2e^{-\gamma}/|k|x)$ as one approaches the distances $x \sim k^{-1}$ (cf. Fig. 5). For $x \gg k^{-1}$ the Bessel function K_0 decays exponentially and we expect a crossover in the excitation profiles from the Coulomb power-

law behavior to an exponential decay. One can also check that the other two equations in the linearized set are satisfied up to first order in k.

For the short-range interaction the linearity of the dispersion relation and the fact that $\partial\mu/\partial x_0 < 0$ imply the chirality of the waves. The wave velocity is determined by $\partial\mu/\partial x_0$, which plays the role of the renormalized velocity in the Luttinger model treatment of the edge excitations. Microscopically this quantity is directly related to the compressibility κ of the edge, which can be viewed as a one-dimensional system of length L and $N = -x_0 L \bar{\rho}$ particles with $\kappa = L/N^2(\partial\mu/\partial N)^{-1} = -(\bar{\rho}x_0^2\partial\mu/\partial x_0)^{-1}$. For $x_0 > 0$ N is minus the number of holes on the edge. The compressibility vanishes when the edge of the static solution is far away from the wall (i.e., at large positive x_0) for which case $\omega \sim k^3$, in agreement with Ref. 12. In the Coulomb case the long-wavelength limit of the dispersion curve is dominated by the logarithmic part so that although $\partial\tilde{\mu}/\partial x_0$ can have either sign the excitations are chiral as before.

IV. STATIC SOLUTIONS FOR A HALL BAR

We go on now to consider the case of a wide and long Hall bar defined by hard walls at $x = \pm W/2$. According to our strategy we first show that again a *family* of static solutions of Eqs. (2a)–(2d) exists. This will now be a *two-parameter* family, which we find by appropriately gluing together two solutions of the single wall case. Assuming that the two solutions correspond to the values of x_0 and μ, which are (x_1, μ_1) and (x_2, μ_2), respectively, and denoting the solutions by superscripts 1 and 2 we set

$$\theta = -x_1 y - \mu_1 t \quad \text{(short range)},$$

$$\theta = -x_1 y - \left(\mu_1 - 2\lambda_c x_2 \ln\frac{L}{W}\right)t \quad \text{(Coulomb)},$$

$$\rho = \rho^{(1)}\left(x + \frac{W}{2}\right)\Theta(-x) + \rho^{(2)}\left(\frac{W}{2} - x\right)\Theta(x), \qquad (11)$$

$$v_x = 0, \quad v_y = v_y^{(1)}\left(x + \frac{W}{2}\right) - v_y^{(2)}\left(\frac{W}{2} - x\right),$$

$$a_0(x) = a_0^{(1)}\left(x + \frac{W}{2}\right) + a_0^{(2)}\left(\frac{W}{2} - x\right) - a_0^{(2)}(W),$$

where Θ is the step function and where we assumed $W \ll L$. The gauge fixing in the present case is achieved through the requirements that a_0 vanishes on the left wall and a_y equals $-W/2$ there. The way θ is modified for the Coulomb interaction reflects the change in the electrochemical potential of one edge due to the electrostatic potential induced by the other. Inserting expressions (11) in the CSLG equations (2a)–(2d) one finds that for the short-range interaction they are satisfied up to exponentially small terms if $W \gg \alpha^{-1}$, where α is the decay constant of the single edge static solution defined previously. In the Coulomb case the set (11) is a static solution accurate up to terms of the order $\lambda_c|x_{1,2}|/W$, which we assume to be small. The quantization of the Hall conductance is seen by integrating Eq. (2b) from

one edge to the other. Restoring the units of dimensions we find that the total current through the bar is

$$I = \nu \frac{e^2}{h} \left[a_0 \left(-\frac{W}{2l} \right) - a_0 \left(\frac{W}{2l} \right) \right]$$

$$= \nu \frac{e^2}{h} \left[\frac{\tilde{\mu}_1 - \tilde{\mu}_2}{e} + 2 \frac{\bar{\rho} e}{\epsilon} (x_2 - x_1) \ln \left(\frac{W}{l} \right) \right] \equiv \nu \frac{e^2}{h} V_{\text{Hall}}.$$

(12)

In the Coulomb case the logarithmic dependence on the width of the bar indicates that for wide samples the current flows predominantly in the bulk.

We note that the sum and the difference of the values of x_1 and x_2 determine the charge of and the current through the sample, respectively. In particular $x_1 = -x_2$ corresponds to the physically relevant neutral Hall bar. For the set of symmetric solutions with $x_1 = x_2$ the edge currents balance each other while the asymmetric solutions ($x_1 \neq x_2$) represent a system through which a net current is flowing.

V. EDGE EXCITATIONS IN A HALL BAR

Turning to the edge excitations in the Hall bar we can now separately use the derivatives of the static solution (11) with respect to either x_1 or x_2 to attempt forming gapless modes *à la* Eq. (7), which will be concentrated *on one or another edge* of the bar and propagating each in an opposite direction. However, this prescription fails to satisfy the RPA equations in the case of the Coulomb interaction. Using, for example, derivatives with respect to x_1 and integrating the linearized continuity equation gives a current in the x direction which, as was explained in the discussion following Eq. (10) and presented in the inset of Fig. 5, does not vanish on the right edge. We will now demonstrate that this problem is cured if the zero mode fields $\partial_{x_0}\rho$, $\partial_{x_0}v_y$, and $\partial_{x_0}a_0$ in the ansatz (7) are taken as linear combinations $\partial_{x_1}\rho + \beta \partial_{x_2}\rho$, etc., of the derivatives of the static solution (11). This ansatz will now describe coupled density waves on opposite edges propagating in the *same* direction. Substituting such combinations into Eq. (6d) and assuming $k \ll W^{-1}$ we find to first order in k the dispersion relation that depends on the mixing coefficient β,

$$\frac{\omega}{k} = -\frac{\partial \tilde{\mu}_1}{\partial x_1} + 2\lambda_c \left[(1 + \beta) \ln \left(\frac{2e^{-\gamma}}{|k|} \right) - \beta \ln W \right]. \quad (13)$$

The current ρv_x, Eq. (10), vanishes on the left wall by construction. The value of β is found by demanding that it will also vanish on the right wall. This condition leads to a quadratic equation in β giving the solutions

$$\beta_\pm = -Z \pm (Z^2 - 1)^{1/2}$$

with

$$Z = \frac{\ln(2e^{-\gamma}/|k|) - (1/4\lambda_c)(\partial \tilde{\mu}_1/\partial x_1 + \partial \tilde{\mu}_2/\partial x_2)}{\ln(2e^{-\gamma}/|k|W)}, \quad (14)$$
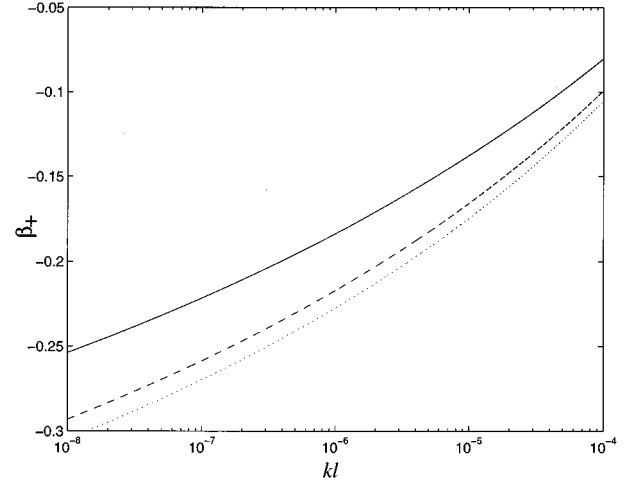
and corresponding dispersion relations

FIG. 6. The mixing coefficient β_+ for a Hall bar of width $W = 1000l$ and Coulomb interaction with $\lambda_c = 0.3$. The results are shown for different values of the current through the bar: $I = 0$ (dotted line), $I = 5.4 e \omega_c$ (dashed line), and $I = 14 e \omega_c$ (solid line).

$$\omega_\pm = -\frac{1}{2} \left(\frac{\partial \tilde{\mu}_1}{\partial x_1} - \frac{\partial \tilde{\mu}_2}{\partial x_2} \right) k \pm 2\lambda_c k \, \ln \left(\frac{2e^{-\gamma}}{|k|W} \right) (Z^2 - 1)^{1/2}.$$

(15)

In the case of the short-range interaction, $\lambda_c \to 0$, these solutions tend to $\beta = 0$ and $-\infty$ corresponding to modes concentrated on either the left or the right edge. The dispersion relations of these modes are the expected $\omega = -(\partial \mu_1/\partial x_1)k$ and $\omega = (\partial \mu_2/\partial x_2)k$. As anticipated the long-range Coulomb forces result in interedge interaction that produces eigenmodes living simultaneously on both edges. This phenomenon has been predicted in Refs. 14 and
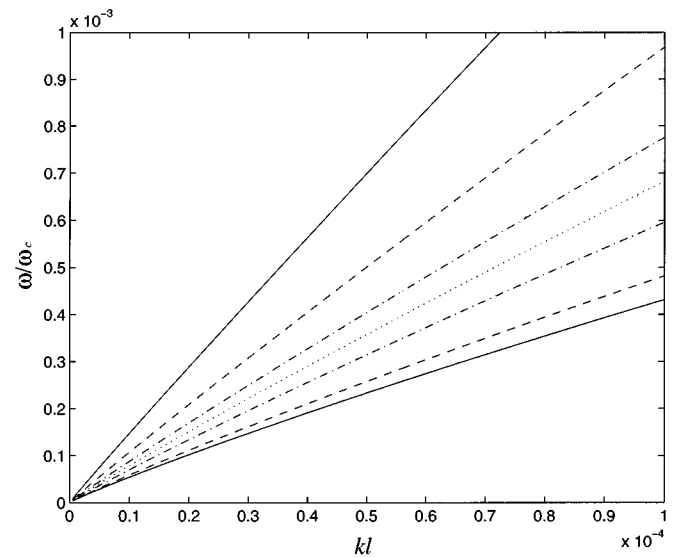

FIG. 7. Dispersion relations for a Hall bar of width $W = 1000l$ and Coulomb interaction with $\lambda_c = 0.3$. The relations are shown for different values of the current through the bar: $I = 0$ (dotted line), $I = 1.8 e \omega_c$ (dashed-dotted line), $I = 5.4 e \omega_c$ (dashed line), and $I = 14 e \omega_c$ (solid line). For each of these cases the upper and lower curves represent ω_+ and $|\omega_-|$, respectively.

10 within the framework of the Luttinger model of the edge excitations in the QHE. It can be interpreted as a Coulomb drag of charges on one edge by the traveling density fluctuations on the other. Indeed $\beta_\pm$ are negative, showing that the edges oscillate out of phase. The effect is the strongest for $k \to 0$ when $\beta_\pm$ tend to $-1 \pm O(|\ln k|^{-1/2})$. For a given mode the direction of propagation of the excitation is determined by the edge with the larger amplitude of charge fluctuations while the presence of the other edge reduces the velocity. For k increasing towards W^{-1} β_+ decreases in magnitude while $\beta_- = \beta_+^{-1}$ changes correspondingly in an opposite manner. This behavior is demonstrated in Fig. 6. Simultaneously the frequencies of the modes approach their single edge values, indicating a decoupling of the edges in this limit.

For a neutral Hall bar sustaining a small current (i.e., small x_1) Eq. (12) may be used to approximate the current (in dimensionless units) by $I \simeq 2x_1(\partial \tilde{\mu}_1/\partial x_1)_{x_1=0}$ $-4\lambda_c x_1 \ln W$. In this region we find numerically that $\partial \tilde{\mu}_1/\partial x_1 \approx a + bx_1$ where $a \approx -1.5 + 0.75(\lambda_c + \lambda_c^2)$ and b is a constant close to unity over the range of λ_c presented in Fig. 3. These observations enable us to rewrite the dispersion relations (15) in the following way:

$$\omega_\pm = \omega_c lk \left\{ \frac{b\pi\nu^{-1}}{2\lambda_c \ln(W/l) - a} \frac{I}{e\omega_c} \right.$$
$$\left. \pm 2\lambda_c \sqrt{\left[\ln\left(\frac{2e^{-\gamma}}{|k|l}\right) - \frac{a}{2\lambda_c}\right]^2 - \ln^2\left(\frac{2e^{-\gamma}}{|k|W}\right)} \right\}. \quad (16)$$

Using this form of the dispersion relations it is apparent that when there is no current flowing in the bar the two modes travel in opposite directions with equal velocities. For a nonzero total current this symmetry is broken and one of the modes is carried with the flow while the other is retarded by it. In Fig. 7 we present dispersion curves for different values of the current. For the range of k used in this figure the mixing between the edges is already quite small (cf. Fig. 6) and the dispersion curves are close to the single edge dispersion relations. For a FQHE sample with a length of 1 mm the typical frequency of these modes is of the order of a few GHz and the relevant scale of the currents is determined by $e\omega_c \simeq 5\ \mu$A. When the current through the bar is large compared to $e\omega_c$ the linear approximation used to derive (16) is no longer applicable. In such cases one should use Eqs. (12) and (15) to obtain an implicit relation between the current and the frequency. The dependence of the dispersion relation on the current suggests the possibility of a parametric excitation of these edge waves by driving an alternating current through the sample. We will report on this mechanism elsewhere.

[1] B. I. Halperin, Phys. Rev. B **25**, 2185 (1982).

[2] M. Büttiker, Phys. Rev. B **38**, 9375 (1988).

[3] C. W. J. Beenakker, Phys. Rev. Lett. **64**, 216 (1990).

[4] D. B. Chklovskii, B. I. Shklovskii, and L. I. Glazman, Phys. Rev. B **46**, 4026 (1992).

[5] X. G. Wen, Int. J. Mod. Phys. B **6**, 1711 (1992).

[6] C. de C. Chamon and X. G. Wen, Phys. Rev. Lett. **70**, 2605 (1993).

[7] C. L. Kane and Matthew P. A. Fisher, Phys. Rev. Lett. **72**, 724 (1994).

[8] S. C. Zhang, H. Hansson, and S. Kivelson, Phys. Rev. Lett. **62**, 82 (1989).

[9] N. Nagaosa and M. Kohmoto, in *Correlation Effects in Low-Dimensional Systems*, edited by A. Okiji and N. Kawakami (Springer-Verlag, Berlin, 1994), p. 168.

[10] Yuval Oreg and Alexander M. Finkel'stein, Phys. Rev. Lett. **74**, 3668 (1995).

[11] Z. F. Ezawa and A. Iwazaki, J. Phys. Soc. Jpn. **61**, 4133 (1992).

[12] S. Giovanazzi, L. Pitaevskii, and S. Stringari, Phys. Rev. Lett. **72**, 3230 (1994).

[13] V. A. Volkov and S. A. Mikhailov, Pis'ma Zh. Éksp. Teor. Fiz. **42**, 450 (1985) [JETP Lett. **42**, 556 (1985)].

[14] X. G. Wen, Phys. Rev. B **44**, 5708 (1991).